объединенный
институт
ядерных
исследований
дубна

E1-90-167

Yu.Ye.Bonyushkin, A.V.Korytov, V.L.Malyshev,
S.Nova*

SPATIAL RESOLUTION OF PLASTIC STREAMER TUBES WITH WIDE STRIP READOUT

Submitted to "NIM"

*Charles University, Prague, Czechoslovakia

1990

1. INTRODUCTION

Plastic Streamer Tubes (PST) [1] are widely used in large scale experiments because of their low cost, flexibility and operation reliability. In particular the possibility of analog readout of strips transverse to the anode wires for precise coordinate measurements makes them well suited for large tracking systems [2]. There is a large list of publications devoted to the spatial resolution of PST achievable with pickup strips. These results are summarized in table 1. The table shows that a strip width usually used for PST with 9×9 mm^2 cell size is about 10 mm. This choice is determined by the width of the induced charge distribution, which is about 10 mm [3] if there is no charge flow along the cathode surface.

However, it should be noted that the resolution in PSTs is worse than for the case of strip readout of usual proportional wire chambers with the similar geometry. For example, in the Ref.[12] the resolution of about 200 μm in the beam was obtained in the chamber with a 4 mm anode-cathode gap and with 8 mm strips. For the case of photon-caused ionization the results obtained with proportional chambers are better as well (e.g. ≤100 μm in the Ref.[13]).

It is natural to assume that a worse resolution is caused by local non-uniformities of the cathode graphiting and by local mechanical deviations which can result in distortions in the induced pulse shape. Thus, a certain broadening of the induced signal, such as the one caused by the integration time increase (fig.1) and/or the cathode resistivity decrease, might allow the use of strips with a larger pitch without deteriorating the spatial resolution or even with improving it as wider strips integrate local non-uniformities.

2. THE EXPERIMENTAL SETUP

We used the standard PST geometry (coverless type) [14]: a plastic profile with a 9×9 mm^2 internal cell inserted in a gas-tight envelope. The profile used for the test tube was one of the profiles made in Frascati for the DELPHI [15] hadron

Table 1

Tube cell, mm	Strip pitch mm	Ionization source	Resolution, µm	Profile/cover resistivity kOhm/sq	Integration time, ns	Ref.
9×9	10	^{55}Fe	<200	~160		[4]
9×9	11	beam	~1300			[5]
15×20	10 20	beam	420-450 440	30-80	1000	[6]
9×9	5 10	beam	600 350	150-200 (coverless)		[7]
9×9	21	cosmic-rays	2100	20-20,000/ /1000		[8]
9×9	12.7	beam	420	<2 (coverless)	t_M=1.86 µs	[9]
9×9	12	^{55}Fe beam	200-400 400-500	30/300	50	[10]
9×9	12.7	beam	700	150 (coverless)	t_M=1.86 µs	[11]

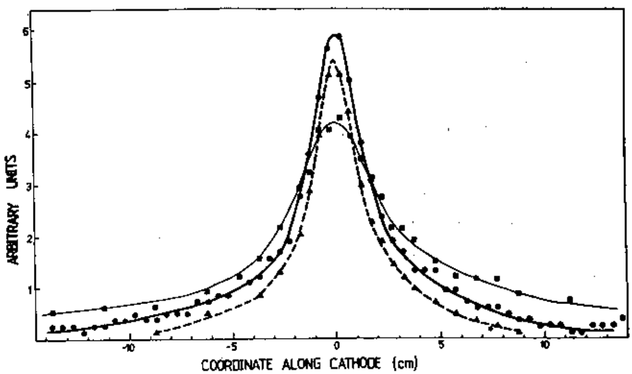

Fig.1 The broadening of the induced charge distribution caused by the increasing integration time (Δ - 50 ns, ∘ - 100 ns, ▪ - 300 ns). The measurements were carried out with 4 mm strips over the 100 kOhm/sq cover. Non-invariance of the total charge summed over all strips is due to the large signal duration (~100 ns).

calorimeter. The anode was a Be-Cu wire 80 μm in diameter. The gas mixture was Ar+isobutane=25%+75%. The singles rate and mean charge versus high voltage for the tested tube are presented in fig.2. The surface resistivity of the bottom of the profile was typically 30 kΩ/sq, while that of the walls between the cells was about 10 kΩ/sq.

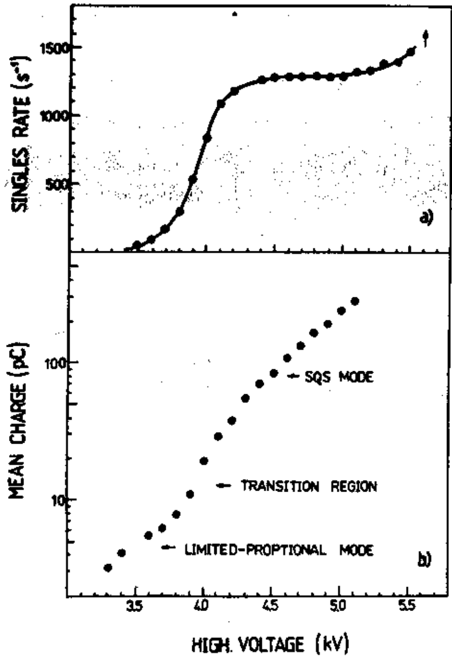

Fig.2 (a) The singles rate (15 mV/50 Ohm threshold, 300 ns shape time) and (b) the mean charge versus high voltage (100 ns integration time) for the tested tube.
The gas mixture Ar+isobutane=25%+75%; ^{90}Sr β-source.

Figure 3 shows a scheme of the whole mechanical arrangement for the measurements. As we planned to carry out the measurements with a β-source, special measures to avoid multiple scattering of soft electrons were taken.

First, the unnecessary substance was removed: the holes in the envelope were made and then were covered with 12 μm mylar (upper side) and thin scotch (lower side); the unnecessary substance from the lower side of the profile and from the lower

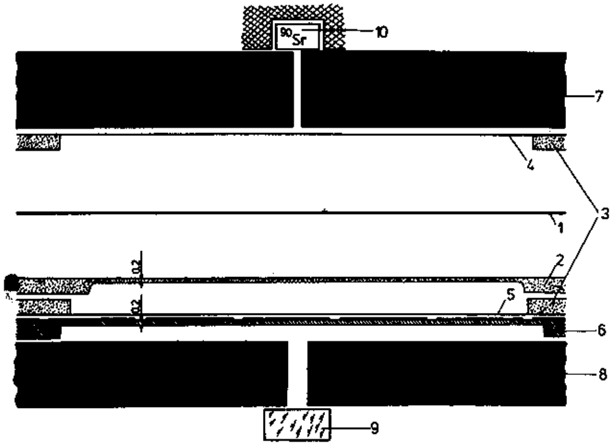

Fig.3 Experimental setup: (1) anode wire; (2) profile; 200 μm thick; (3) penal with holes; (4) 12 μm mylar; (5) 60 μm scotch; (6) strip board, 200 μm thick; (7) upper collimator, 30 mm thick, Cu; (8) lower collimator, 30 mm thick, Cu; (9) scintillator; (10) β-source.

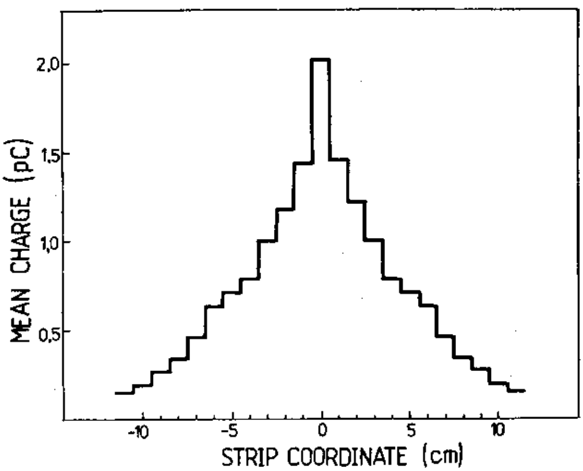

Fig.4 Relative charge distribution over the 1 cm wide strips for the tested tube.

side of the strip board was removed as well. Secondly, the narrow upper collimator (500 μm slit) and the lower collimator (1.8 mm slit) were used to select straight tracks by the coincidence of signals from the tube and the scintillator placed under the lower collimator. The upper collimator and the lower collimator were mechanically connected and it was possible to move them along the tube with ~50 μm precision. The track uncertainty determined by the geometry of the upper collimator was ~200 μm (RMS).

The strip board was placed on the side of the profile. The strip signals were amplified and then connected to the inputs of the 8-bit ADC (the integration time was 100 ns). In all measurements the amplifier noise was considerably smaller than one channel width of the ADC.

Fig.4 shows the charge distribution over the 1 cm wide strips. Clearly, at chosen resistivity and integration time the charge flow on the resistive cathode plays an important role.

3. RESULTS

To reconstruct the track position the centre of gravity method was used. We confined ourselves to a maximum of six strips for COG weighting to reconstruct the track position. It is well known that almost all simple methods of position reconstruction (COG, interpolations by Gaussian, Lorentzian, parabolic functions etc.) result in systematic shifts [3,12].

Moving the collimators along the tube we thoroughly measured the dependence of the centre of gravity coordinate on the real coordinate of the track (this permitted all systematics to be taken into account). The example of a such dependence is presented in fig.5a. Fig.5b presents the derivative $\frac{dx_{cog}}{dx_{real}}$ needed for the reconstructions of the real spatial resolution:

$$\sigma_{real}=\sigma_{cog}/\left(\frac{dx_{cog}}{dx_{real}}\right).$$

Five strip pitches (10,20,30,40,50 mm) were used in the measurements. In each case the strips were separated by 1 mm spaces.

The measurements were performed in the following way. The histograms of COG coordinates were accumulated for different positions of the collimators. Six, five, four and three strips were used for the COG calculations. Then these histograms were fitted by a Gaussian function. The standard deviations σ_{cog}

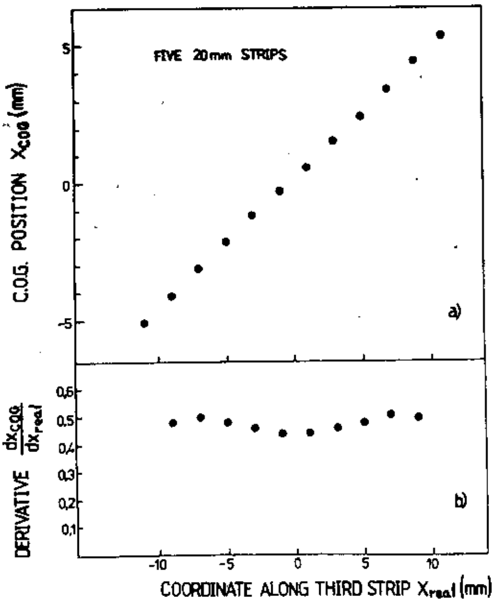

Fig.5 (a) Dependence of the centre of gravity coordinate x_{COG} on the real coordinate of the track x_{real} and (b) the derivative $\frac{dx_{COG}}{dx_{real}}$ obtained for 2 cm strip pitch.

obtained in these fits were divided by the corresponding derivatives $\frac{dx_{COG}}{dx_{real}}$ to obtain the estimations of the real position resolutions $\sigma_{real}=\sigma_{COG}/\left(\frac{dx_{COG}}{dx_{real}}\right)$. Fig.6 demonstrates examples of the achievable resolution.

The overall results obtained with the odd (5) and even (6) number of strips for the COG analysis are presented in fig.7. The results obtained with the smaller number of strips were systematically worse or of the same order. The use of an odd and even number of strips is essential for two reasons. First, if the number of strips for the position analysis is fixed and, for example, even, then the uncertainty in the choice of a strip group for tracks passed in the vicinity of a strip centre will appear, which may result in the deterioration of the spatial resolution. And secondly, as seen from fig.7, even in the case of a correct choice of a strip group, the best resolution is achieved when a track passes through the centre of a strip group.

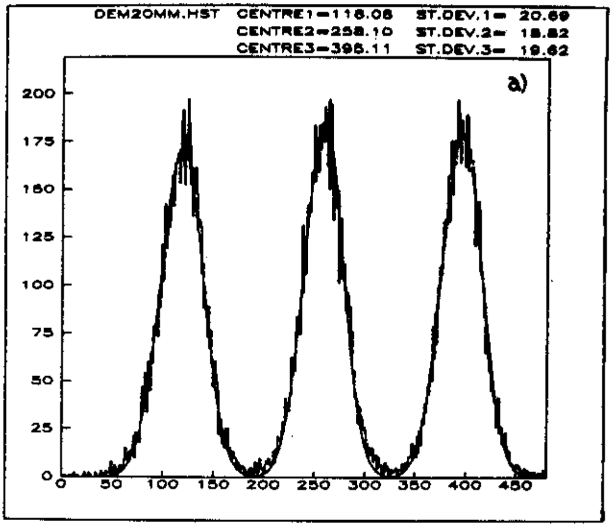

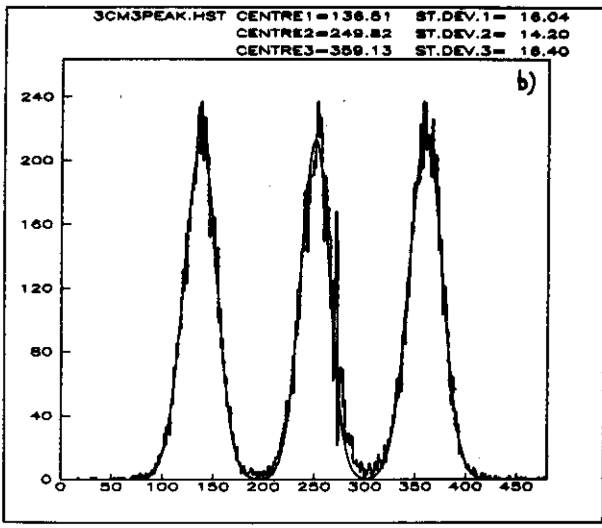

Fig.6 The histograms of induced charge distribution centroids for three slit positions, 3 mm apart. The results are obtained by the centre of gravity method with readout from: (a) six 20 mm strips, (b) five 30 mm strips. The resolution for these two particular cases is about 370 μm after quadratical subtraction of ~200 μm track uncertainty.

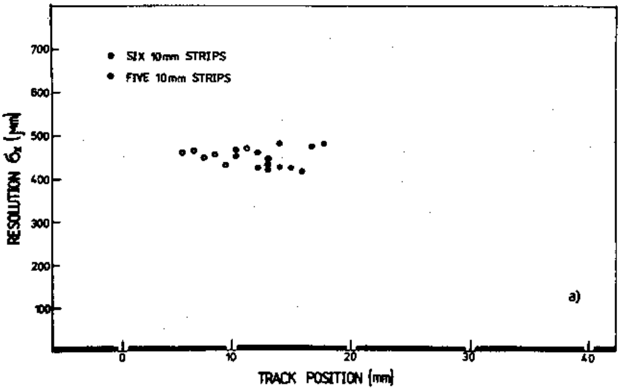
SIX 10mm STRIPS
FIVE 10mm STRIPS
RESOLUTION σx (μm)
TRACK POSITION (mm)
a)

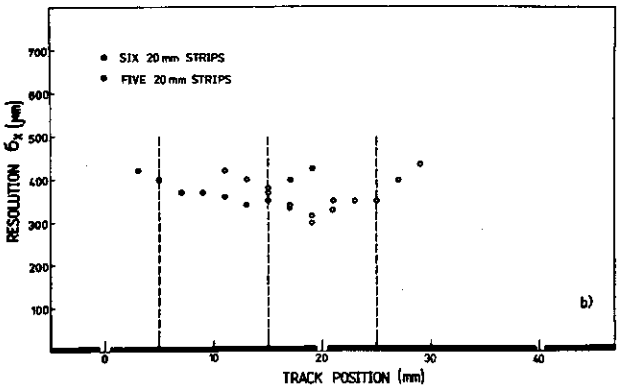
SIX 20mm STRIPS
FIVE 20mm STRIPS
RESOLUTION σx (μm)
TRACK POSITION (mm)
b)

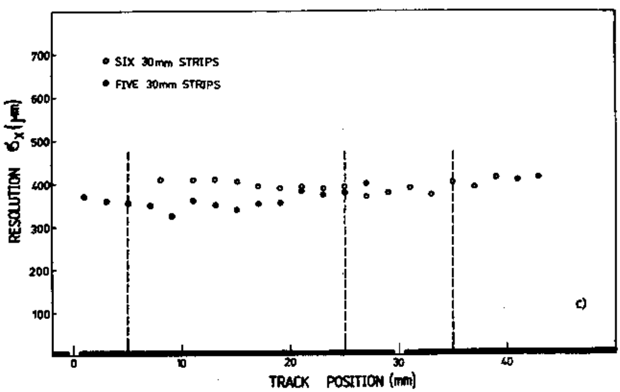
SIX 30mm STRIPS
FIVE 30mm STRIPS
RESOLUTION σx (μm)
TRACK POSITION (mm)
c)

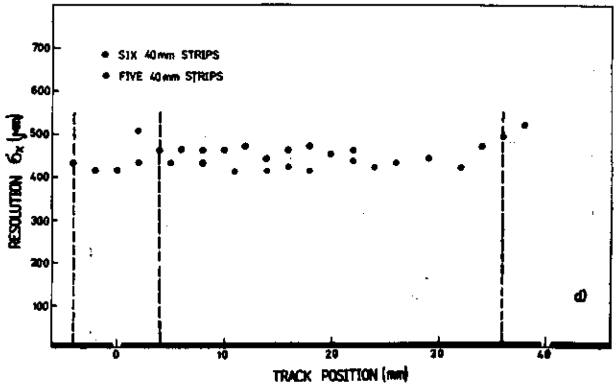

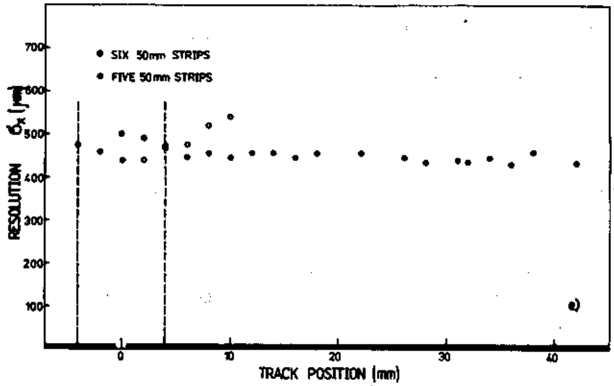

Fig.7 Spatial resolutions obtained after quadratical subtraction of ~200 μm track uncertainty as a function of the track position relative to the strip for different strip pitches: (a) 10 mm, (b) 20 mm, (c) 30 mm, (d) 40 mm, (e) 50 mm.

Thus, to obtain a good averaged spatial resolution it is reasonable to use an odd and even number of strips for the position analysis for tracks traversing the central region of a strip and the region between strips respectively.

The resolutions averaged over the whole strip pitch are shown in fig.8. The results obtained with five and six strips were used to perform the averaging. The dashed lines in fig.7 divide the strip pitches into regions where five or six strips should be used for the COG calculations.

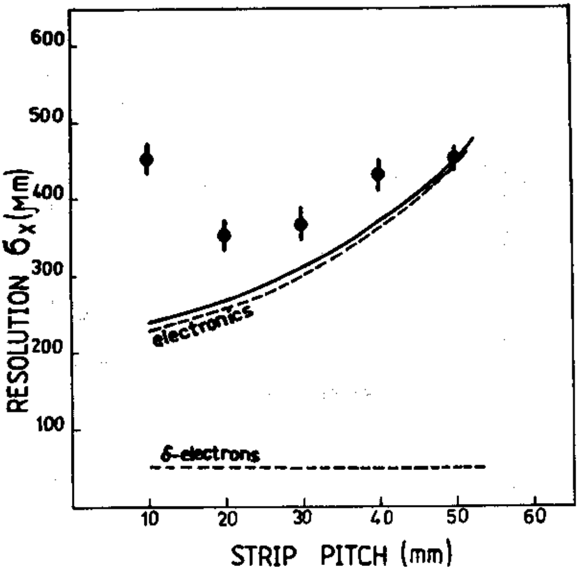

Fig.8 Spatial resolution averaged over a strip versus a strip pitch. The averaging is explained in the text.

The solid line in fig.8 shows quadratically added contributions to the spatial resolution of the electronics and δ-electrons (the dashed lines).

To evaluate the electronic contribution to the spatial resolution we used the usual method [17]: first, the shape of the induced charge distribution (fig.4) permits the derivative $\frac{dx_{coa}}{dx_{real}}$ to be estimated and, secondly, considering the uncertainty connected with the finite bin width of the 8-bit ADC as the main electronic error, one can easily estimate the value of σ_{coa}. The ratio $\sigma_{coa}/\left(\frac{dx_{coa}}{dx_{real}}\right)$ gives the estimation of σ_{real}.

The contribution of δ-electrons was estimated to be about 50 μm (the best results obtained for MWPC with a ~10 mm gas gap, using the analog strip readout [16]) and it is negligible as compared with the electronic contribution.

Fig.8 shows that the narrower strips the more discrepancy between expected and experimental resolutions. This is most probably due to the local non-uniformities of the cathode resistivity, which can cause local distortions in the induced pulse shape.

4. CONCLUSIONS

We tested a streamer tube chamber with the analog readout of strips transverse to the anode wires. The tests allow the conclusion that the spatial resolution better than 400 μm is achievable in PST with a rather wide strip pitch (~3 cm). Such a wide pitch, being almost 3 times larger than a usual one, allows one to decrease the total number of strips per unit length and consequently the cost of the electronics.

The method is based on the broadening of the induced charge distribution caused by the low cathode resistivity and/or the large integration time.

This method is the best when low particle multiplicity is expected, as in muon detectors.

Acknowledgements

The authors are grateful to G.V.Micelmacher for the support of this work. We thank G.D.Alekseev and A.G.Olshevski for the fruitful discussions, T.Todorov and Yu.V.Sedykh for the softwear consultations. We would like to thank G.Karpenko who performed almost whole mechanical work.

References

[1] E.Iarocci, NIM 217(1983)30.
[2] CHARM II collaboration, CERN/SPSC/83-24 (1983);
UA1 collaboration, CERN/SPSC/82-51 (1982);
H1 Collaboration, Letter of Intent for an experiment at HERA, DESY (June 28, 1985);
ZEUS Collaboration, ZEUS a detector for HERA, DESY (June 1985).
[3] I.Endo et al., NIM 188(1981)51.
[4] G.Battistoni et al., NIM 176(1980)297.
[5] M.Bourquin and T.Modis, NIM 217(1983)201.
[6] J.Fujimoto et al., NIM A252(1986)53.
[7] G.D'Agostini et al., NIM A252(1986)431.
[8] J.P.De Wulf et al., NIM A252(1986)443.
[9] A.Bettini et al., CERN-EP/86-162.

[10] G.Bauer et al., NIM A260(1987)101.
[11] F.Gasparini et al., NIM A273(1988)485.
[12] N.Awaji et al., NIM 198(1982)243.
[13] T.Miki et al., NIM A236(1985)64.
[14] G.Battistoni et al., NIM 217(1983) 429.
[15] DELPHI, Technical Proposal, CERN/LEPS/83-66/1.
[16] G.Charpak et al., NIM 167(1979)455.
L.S.Barabash et al., NIM A236(1985)271.
[17] E.Gatti et al., NIM 163(1979)83.

Received by Publishing Department
on March 7, 1990.